presented a feedback control law that globally and asymptotically stabilizes a spacecraft about a revolute motion along a specified inertial axis. After the spacecraft is stabilized, the command inputs of the feedback control law oscillate periodically to conserve the system angular momentum. In general there is no feedback control law that can detumble and reorient the spacecraft simultaneously.

References

[1]Kim, S., and Kim, Y., "Sliding Mode Stabilizing Control Law of Underactuated Spacecraft," *Proceedings of the AIAA Guidance, Navigation, and Control Conference* [CD-ROM], AIAA, Reston, VA, 2000.

[2]Tsiotras, P., and Longuski, J. M., "Spin-Axis Stabilization of Symmetric Spacecraft with Two Control Torques," *Systems and Control Letters*, Vol. 23, No. 6, 1994, pp. 395–402.

[3]Crouch, P. E., "Spacecraft Attitude Control and Stabilization: Applications of Geometric Control Theory to Rigid Body Models," *IEEE Transactions on Automatic Control*, Vol. 29, No. 4, 1984, pp. 321–331.

[4]Krishnan, H., McClamroch, N. H., and Reyhanoglu, M., "Attitude Stabilization of a Rigid Spacecraft Using Two Momentum Wheel Actuators," *Journal of Guidance, Control, and Dynamics*, Vol. 18, No. 2, 1995, pp. 256–263.

[5]Junkins, J. L., and Turner, J. D., *Optimal Spacecraft Rotational Maneuvers*, Elsevier, Amsterdam, 1986, p. 275.

[6]Tsiotras, P., and Longuski, J. M., "A New Parameterization of the Attitude Kinematics," *Journal of Astronautical Sciences*, Vol. 43, No. 3, 1995, pp. 243–262.

[7]Khalil, H. K., *Nonlinear Systems*, 2nd ed., Prentice–Hall, Englewood Cliffs, NJ, 1996, p. 113.

Uniform Damping of Plates Using a Modified Nodal Control Method

Jun-Kyung Song* and Gregory Washington†
The Ohio State University, Columbus, Ohio 43210-1107

I. Introduction

THE ultimate goal of many vibration control schemes is to dampen all of the active modes participating in the system response. In addition, one may want to preserve the uncontrolled mode shapes and frequencies. The main advantage in doing this lies in the energy savings that accompanies modal preservation. Finally, one may want an analytically sound method for actuator and sensor placement. Toward this end, the natural control theory provides a means for damping a structure, whereas preserving the modes and the node control theory provides a means for actuator and sensor placement.[1–3] Weaver and Silverberg applied this combination to actively damp a beam.[4] The strategy states that one can control the lowest N modes participating in a response by placing discrete sensor/actuator pairs at the nodes of the $(N+1)$ mode.[4] In doing this there is a natural decoupling that leads to a controlled system with the following properties: 1) frequency and modal invariance and 2) uniform damping.[4] Washington and Silverberg[5] added bias or steady-state calibration to this work, and Rosetti and Sun[6] extended the work to rings. Although the node control theory has been used extensively in beams and rings, a general proof of the theory was not discussed until recently.[7,8] Now that there is a mathematical basis for this theorem, its application to plates, shells, and general problems can now be investigated. The work in this Note applies the theory to rectangular plates. There are a myriad of uses associated with uniform damping nodal control (UDNC) as it applies to aircraft structures because the boundary condition of dominant local vibration of the aircraft can be modeled as combination of fixed and simply supported (SS) boundary conditions. Two important contributions are actuator placement for active noise cancellation in aircraft cabin enclosures and actuator placement for vibration control of next generation flexible aircraft structures.

In its application to plates, the work in this study postulates that the lowest M and N modes of vibration are controlled by $M \times N$ pairs of discrete actuators/sensors located at the intersections of the nodal lines of the $(M+1)\times(N+1)$ mode. The overall benefits of the method are as follows: 1) discrete sensors and actuators are used instead of distributed modal sensors and actuators.[9–11] 2) The method is resistant to control spillover[4,5] because the actuator/sensor pairs are located at the nodes of the next highest mode, which diagonalizes the control matrices. 3) Control moves are not calculated in modal domain but in the physical domain. 4) All modes are designed to be damped at the same rate thereby conserving energy. 5) The closed-loop frequencies are equivalent to open-loop frequencies. 6) The original mode shapes of the system are preserved. This work begins with the application of UDNC to SS plates. The methodology is then applied to the clamped-simply supported-clamped-simply supported (C-SS-C-SS) case. The Ritz method is then used to handle cases where an analytical solution does not exist. The paper then concludes with discussion.

II. Uniform Damping Control Method

A. Uniform Damping Control of Plates with Distributed Actuators/Sensors

The control term $f(x, y, z)$ is presented in the right-hand side of the following governing equation for rectangular plates:

$$\rho\frac{\mathrm{d}^2 w(x,y,t)}{\mathrm{d}t^2} + D\nabla^4 w(x,y,t) = f(x,y,t) \tag{1}$$

In Eq. (1) the displacement field and excitation terms can be written by the eigenfunction superposition method[12] as the following:

$$w(x,y,t) = \sum_m^\infty \sum_n^\infty W_{mn}(x,y)\eta_{mn}(t) \tag{2}$$

$$f(x,y,t) = \sum_m^\infty \sum_n^\infty W_{mn}(x,y) f_{mn}(t) \tag{3}$$

$$f_{mn}(t) = \iint_{x\ y} W_{mn}(x,y) f(x,y,t)\,\mathrm{d}x\,\mathrm{d}y \tag{4}$$

where the subscripts m and n represent the mth mode in the x direction and nth mode in the y direction. The control force is expressed as

$$f(x,y,t) = g w(x,y,t) + h\dot{w}(x,y,t) \tag{5}$$

where g and h are the uniform damping coefficients.[12] The g and h coefficients are proportional to the measured displacement and velocity, respectively. Uniform damping control for each individual mode can be obtained by employing the principles of uniform damping[3] into Eq. (4):

$$f_{mn}(t) = \iint_{x,y} W_{mn} g \sum_r \sum_s W_{rs}\eta_{rs}(t)\,\mathrm{d}x\,\mathrm{d}y + \iint_{x,y} W_{mn} h \sum_r \sum_s W_{rs}\dot{\eta}_{rs}(t)\,\mathrm{d}x\,\mathrm{d}y \tag{6}$$

Substituting Eqs. (2–4) into Eq. (1), utilizing Eq. (6), and applying the two-dimensional orthonormality relationships yields the following equation:

$$\ddot{\eta}_{mn}(t) + \lambda_{mn}\eta_{mn}(t) = g\eta_{mn}(t) + h\dot{\eta}_{mn}(t) \tag{7}$$

If distributed sensors and actuators are used, the resulting gain matrix of the preceding equation can be shown to be diagonal. Here M and N are the largest number of modes considered to participate in the system in the x and y directions, respectively. When discrete actuators and sensors are used; however, the control gain matrices

Received 20 February 2001; revision received 23 April 2001; accepted for publication 24 April 2001.

*Research Associate, Intelligent Structures and Systems Laboratory.
†Associate Professor, Intelligent Structures and Systems Laboratory.

in Eq. (6) are not diagonal, and this produces the effect of modal coupling. The novelty of this work is that UDNC applied to plates eliminates this issue, even when the actuators are discrete.

B. UDNC on the Plate with $M \times N$ Pairs of Actuators/Sensors

In this section we discuss how discrete sensors and actuators affect the control gain matrices. In this formulation $M \times N$ number of actuator/sensor pairs are needed to control $M \times N$ modes in the x and y direction, respectively. It will be shown that the locations are determined at the intersections of the $(M+1)$ mode nodal lines and the $(N+1)$ mode nodal lines. Because the forces are discrete, the forcing term in the governing equation (1) is expressed as:

$$f(x,y,t) = g_i \sum_{i}^{M\times N} w\left(x_i^*, y_i^*, t\right)\delta\left(x - x_i^*\right)\delta\left(y - y_i^*\right) + h_i \sum_{i}^{M\times N} \dot{w}\left(x_i^*, y_i^*, t\right)\delta\left(x - x_i^*\right)\delta\left(y - y_i^*\right) \tag{8}$$

where i indicates the ith sensor/actuator pair and x^* and y^* represent the location of sensors and actuators. Multiplying the preceding equation by $W_{\rm rs}$, integrating over the length, and utilizing orthonormality produces the following equations:

$$\iint \sum_{i}^{M\times N} W_{\rm rs}(x,y)\delta\left(x - x_i^*\right)\delta\left(y - y_i^*\right)g_i \times \sum_m \sum_n W_{mn}(x^*, y^*)\eta_{mn}(t)\,{\rm d}x\,{\rm d}y = \sum_{i}^{M\times N} W_{\rm rs}(x^*, y^*)g_i \sum_m \sum_n W_{mn}(x^*, y^*)\eta_{mn}(t) \tag{9a}$$

$$\iint \sum_{i}^{M\times N} W_{\rm rs}(x,y)\delta\left(x - x_i^*\right)\delta\left(y - y_i^*\right)h_i \times \sum_m \sum_n W_{mn}(x^*, y^*)\dot{\eta}_{mn}(t)\,{\rm d}x\,{\rm d}y = \sum_{i}^{M\times N} W_{\rm rs}(x^*, y^*)h_i \sum_m \sum_n W_{mn}(x^*, y^*)\dot{\eta}_{mn}(t) \tag{9b}$$

Conducting the same process as in the preceding section, the UDNC forces for the mnth mode are obtained as the following:

$$\sum_{i}^{M\times N} f_{mn,i}(t) = \sum_{i}^{M\times N} \left\{ W_{mn}\left(x_i^*, y_i^*\right)g_i \sum_r \sum_s \left[W_{\rm rs}\left(x_i^*, y_i^*\right)\eta_{\rm rs}(t)\right]\right\} + \sum_{i}^{M\times N} \left\{ W_{mn}\left(x_i^*, y_i^*\right)h_i \sum_r \sum_s \left[W_{\rm rs}\left(x_i^*, y_i^*\right)\dot{\eta}_{\rm rs}(t)\right]\right\} \tag{10}$$

where the indexes m and r change from 1 to M and n and s change from 1 to N. The equations for each mode are rearranged as

$$\ddot{\eta}_{mn}(t) + \lambda_{mn}\eta_{mn}(t) = \sum_{i}^{M\times N} f_{mn,i} \tag{11}$$

The fully populated control gain matrices presented in the preceding equation will be diagonalized by proper selection of actuators and sensors locations. We will see that the proper choice results in the exact locations that one would get by applying UDNC.

To illustrate this, let us employ the theory on a simple system. Toward that end, we will damp a SS rectangular plate up to the 2×1 mode. The mode shape and normalized natural frequencies are the following:

$$W(x,y) = \sum_{m}^{\infty}\sum_{n}^{\infty} \sin\frac{m\pi x}{a}\sin\frac{n\pi y}{b}$$

$$\omega_{mn} = \sqrt{\frac{D}{\rho}}\left\{\left(\frac{m\pi}{a}\right) + \left(\frac{n\pi}{b}\right)\right\} \tag{12}$$

Using Eqs. (10) and (12), the proportional control gain matrix (G matrix) is constructed by the following:

$$G = \begin{bmatrix} G_{11} & G_{12} \\ G_{21} & G_{22} \end{bmatrix} \tag{13a}$$

where

$$G_{11} = g_1\left[\sin\left(\frac{\pi a_1}{a}\right)\sin\left(\frac{\pi y}{b}\right)\right]^2 + g_2\left[\sin\left(\frac{\pi a_2}{a}\right)\sin\left(\frac{\pi y}{b}\right)\right]^2 \tag{13b}$$

$$G_{12} = G_{21} \tag{13c}$$

$$G_{21} = g_1\left[\sin\left(\frac{\pi a_1}{a}\right)\sin\left(\frac{\pi y}{b}\right)\sin\left(\frac{2\pi a_1}{a}\right)\sin\left(\frac{\pi y}{b}\right)\right] + g_2\left[\sin\left(\frac{\pi a_2}{a}\right)\sin\left(\frac{\pi y}{b}\right)\sin\left(\frac{2\pi a_2}{a}\right)\sin\left(\frac{\pi y}{b}\right)\right] \tag{13d}$$

$$G_{22} = g_1\left[\sin\left(\frac{2\pi a_1}{a}\right)\sin\left(\frac{\pi y}{b}\right)\right]^2 + g_2\left[\sin\left(\frac{2\pi a_2}{a}\right)\sin\left(\frac{\pi y}{b}\right)\right]^2 \tag{13e}$$

where a_1 and a_2 are the locations of the two actuator/sensor pairs and the gains g_1 and g_2 represent the gains of the actuators at points a_1 and a_2, respectively. First we will calculate the actuator/sensor pair locations in the x direction. Because the mode shapes in the x direction are symmetric and antisymmetric for even and odd modes, respectively, the locations a_1 and a_2 are selected symmetrically with respect to the center. This means $a_2 = (a - a_1)$ where a is the total length in the x direction. To make the control gain matrix uniformly diagonal, $G_{12} = 0$, and $G_{11} = G_{22}$. Applying these issues along with $a_2 = (a - a_1)$ and utilizing trigonometric relationships yield the following equation:

$$g_1 \sin\left(\frac{\pi a_1}{a}\right)\sin\left(\frac{2\pi a_1}{a}\right) - g_2 \sin\left(\frac{\pi a_1}{a}\right)\sin\left(\frac{2\pi a_1}{a}\right) = 0 \tag{14}$$

Uniform damping is achieved when the coefficient g is a constant for all different actuators. This means g_1 and g_2 are both equal to a constant g. Second, the actuator locations a_1 and a_2 generating the uniform control gains are determined by substituting Eqs. (13) and (14) and utilizing the trigonometric relationships:

$$\sin(3\pi a_1/2a)\sin(\pi a_1/2a) = 0 \tag{15}$$

The solutions of the preceding equation in the range of $0 < a_1 < a$ are $a_1 = \frac{2}{3}\cdot a$ and $a_2 = \frac{1}{2}\cdot a$. Similarly, the location of actuator in the y direction is calculated from Eq. (12) as $\cos(2\pi y/b) = 1$. The solution of the equation in the range of $0 < b_1 < b$ is $b_1 = b/2$. Remarkably, the results are the intersections of the 3×2 mode nodal line presented in Fig. 1. Remember the UDNC law states that we place our actuators at the intersection of the $(M+1)\times(N+1)$ nodal lines to control the $(M)\times(N)$ mode. It was postulated that the correct placement of actuator/sensor pairs were at the intersection of the nodal lines. As presented in this example, the coefficients and actuator locations to generate uniformly diagonal matrices are identical to the coefficients and locations determined by UDNC theory. The following equation is obtained for the proportional control gain matrix[3,4] of the example by substituting the preceding results into Eq. (13):

$$G = \tfrac{4}{3}g[I]_{2\times 2}, \qquad H = (2/\alpha)G \tag{16}$$

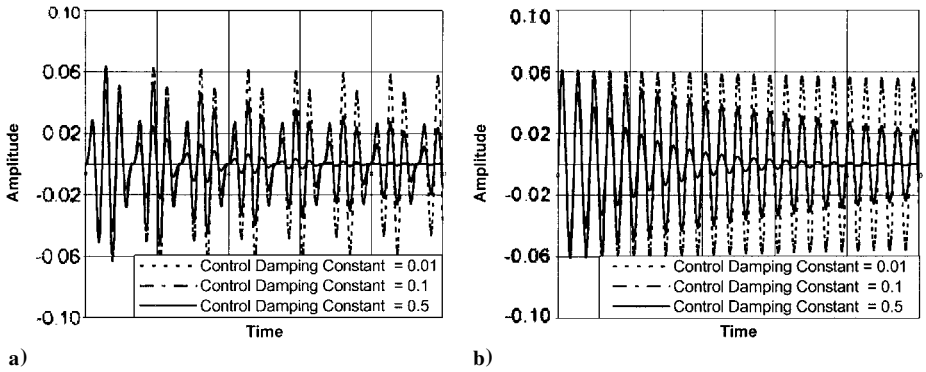

Fig. 1 UDNC on plate with excitation at a) P_1 and b) P_2.

where $[I]$ is identity matrix. As presented in the preceding equation, the gain matrices G and H are uniformly diagonal. To highlight the modal preservation capability of this algorithm, we will show additional simulation results of UDNC on the plate with several different excitation points. The selected locations for the impulse excitation points are $P_1(5a/12, 3b/8)$, $P_2(a/2, b/2)$, and the corresponding responses are presented in Fig. 1. The point of observation is $(2a/3, b/2)$. The selected control damping constant α is given by 0.01, 0.1, and 0.5, and the responses according to the selection are presented in the plots. When the control damping constant α is 0.01, the system response is close to the behavior of the open-loop system. Because the contribution factor of each mode depends on the excitation locations, the cases show different closed-loop response profiles. In Fig. 1a the contribution of multiple modes are present in the total system response. The response presented in Fig. 1b shows one dominant mode response without the contribution of any other mode because the excitation point p_3 is a node of the W_{21} mode and an antinode of W_{11}. The contribution factor of the fundamental mode W_{11} to the total system response is maximized while the contribution factor of the W_{21} mode is nullified. This highlights the fact that modal decoupling can happen with the proper actuator placement prescribed by UDNC. It is clearly shown that a higher control damping constant α induces less settling time and that the damped natural frequencies are not varying as designed by UDNC. We can also see that all active modes are damped at the same rate. This concept has been demonstrated for higher modes as well.

III. UDNC Applied to Various Boundary Conditions

A. SS Rectangular Plates

The next case will present UDNC for a rectangular plate that is SS on all four sides. We will be controlling up to the 2×3 $(M \times N)$ mode. The locations for the sensor/actuator pairs are the intersections of the nodal lines of the third and fourth modes in x and y coordinates, respectively. The locations are calculated as follows and are presented in Fig. 2a:

$$x_1^* = a/3, \qquad x_2^* = 2a/3, \qquad y_1^* = b/4$$
$$y_2^* = 2b/4, \qquad y_3^* = 3b/4 \tag{17}$$

Substituting Eq. (13) and the solution for SS plates given by the Eq. (12) into the control gain matrix in Eq. (10) yields following diagonalized G matrix. The H matrix is obtained in a similar manner:

$$G = 3.0 \cdot g \cdot [I]_{6\times 6}, \qquad H = (2/\alpha)G \tag{18}$$

As presented in these two examples, the UDNC method produces diagonalized uniform control gain matrices.

B. C-SS-C-SS Rectangular Plates

In an earlier section the validity of UDNC has been proven, and simulation results of simple cases were presented. Now, we move on to more general cases of rectangular plates such as C-SS-C-SS. In this section the analytical solution of C-SS-C-SS rectangular plates and the utility of UDNC will be demonstrated. The results will be compared with those obtained by an approximation method in a later section. The boundary conditions for the clamped sides can be expressed as

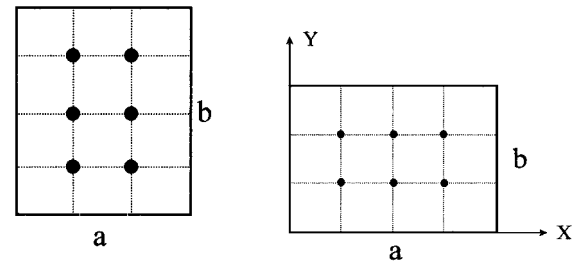

Fig. 2 Location of actuators and sensors.

$$W(x,0) = \frac{\partial W}{\partial y}(x,0) = W(x,b) = \frac{\partial W}{\partial y}(x,b) = 0 \tag{19}$$

The preceding equation produces four homogeneous equations by applying the boundary conditions to the general solution satisfying the SS side boundary condition.[12] These equations can be solved to give the following[12]:

$$W(x,y) = \left\{ \sin\lambda_1 y + \frac{[\lambda_1 \sinh\lambda_2 b - \lambda_2 \sin(\lambda_1 b)](\cos\lambda_1 y - \cosh\lambda_2 y)}{\lambda_2(\cos\lambda_1 b - \cosh\lambda_2 b)} - \frac{\lambda_1 \sinh\lambda_2 y}{\lambda_2} \right\} \sin\alpha x \tag{20}$$

where $\lambda_1 = \sqrt{(k^2 - \alpha^2)}$ and $\lambda_2 = \sqrt{(k^2 + \alpha^2)}$.

The mode shape of an individual mode will be found by substituting the coefficient k_{mn}, a, and b into the preceding equation. The orthogonal mode shapes are orthonormalized by applying the Gram–Schmidt method. The nondimensional frequency parameter is defined as $\lambda^2 = \omega^2 b^4 \rho / D$. The calculated nondimensional frequency parameters are presented in Table 1. The first step is to determine up to what modes you want to damp. In this case we will control up to the 3×2 mode or modes (W_{11}, W_{21}, W_{31}, W_{12}, W_{22}, W_{32}). The next step is to find the locations for the actuator/sensor pairs (Fig. 2b). The dimensions of the plate are 1×0.5 units in the x and y directions, respectively. The UDNC theory states that the actuator/sensor pairs should be at the nodes of $(M+1)$ and $(N+1)$ mode. The locations will be found at the zeros of the fourth mode in the x direction and the third mode in the y direction. The coordinates are the following:

$$x_1 = \tfrac{1}{4}, \qquad x_2 = \tfrac{2}{4}, \qquad x_3 = \tfrac{3}{4}$$
$$y_1 = 0.177063, \qquad y_2 = 0.322936 \tag{21}$$

Table 1 Nondimensional frequency parameters

x index / y index	1	2	3	4
1	$\lambda_{11} = 23.81562612$	$\lambda_{21} = 28.95085036$	$\lambda_{31} = 39.08924660$	$\lambda_{41} = 54.74307074$
2	$\lambda_{12} = 63.53450089$	$\lambda_{22} = 69.32701373$	$\lambda_{32} = 79.52512027$	$\lambda_{42} = 94.58527817$
3	$\lambda_{13} = 122.9296309$	$\lambda_{23} = 129.09553715$	$\lambda_{33} = 139.62234634$	$\lambda_{43} = 154.77570360$
4	$\lambda_{14} = 201.9815976$	$\lambda_{24} = 208.39171967$	$\lambda_{34} = 219.20715560$	$\lambda_{44} = 234.58545320$

Table 2 Nondimensional frequency parameters by the Ritz method

x index / y index	1	2	3	4
1	$\lambda_{11} = 23.81562612$	$\lambda_{21} = 28.95085046$	$\lambda_{31} = 39.09275811$	$\lambda_{41} = 54.78521177$
2	$\lambda_{12} = 63.53450098$	$\lambda_{22} = 69.32701386$	$\lambda_{32} = 79.52738644$	$\lambda_{42} = 94.61591534$

Once the mode shapes and locations of the actuator/sensor pairs are calculated, the following process is straightforward as presented in earlier section. The control gain matrices G and H are obtained as follows:

$$G = g \times \begin{bmatrix} 27.6019 & 0 & 0 & 0 & 0 & 0 \\ 0 & 28.8075 & 0 & 0 & 0 & 0 \\ 0 & 0 & 27.5777 & 0 & 0 & 0 \\ 0 & 0 & 0 & 28.4826 & 0 & 0 \\ 0 & 0 & 0 & 0 & 27.5282 & 0 \\ 0 & 0 & 0 & 0 & 0 & 28.0032 \end{bmatrix}$$

$$H = \frac{2}{\alpha} G \tag{22}$$

As just presented, the UDNC method has uniformly diagonal control gain matrices for this case. This means that the SS-C-SS-C plate will be controlled having all of the merits associated with the UDNC method.

IV. UDNC via the Ritz Method

Because the analytical solutions of many plate vibration problems are difficult if not impossible to find, approximation methods are usually used. In this section we will apply the UDNC a method based on the approximated mode shape obtained by the well-known Ritz method.[13] The algebraic form of displacement function $W(x, y)$, which satisfies the boundary conditions of the structure, is assumed as the following equation:

$$W(x, y) = x(x-a)y^2(y-b)^2 \sum_{i=0}^{I} \sum_{j=0}^{J} A_{ij} x^i y^j \tag{23}$$

where the $I = J = 7$ is selected in this study. The functional can be constructed as follows:

$$L = T - V \tag{24}$$

where the T and V are the maximum values of kinetic energy and potential energy in a vibratory cycle, respectively. These kinetic and potential energies can be represented by the following equations in classical plate vibration theory:

$$V = \frac{D}{2} \iint_{\text{area}} \left\{ (\nabla^2 w)^2 - 2(1-\nu) \left[\frac{\partial^2 w}{\partial x^2} \frac{\partial^2 w}{\partial y^2} - \left(\frac{\partial^2 w}{\partial x \partial y} \right)^2 \right] \right\} \mathrm{d}x\, \mathrm{d}y \tag{25}$$

$$T = \frac{1}{2} \iint_{\text{area}} \rho h \left(\frac{\partial w}{\partial t} \right)^2 \mathrm{d}x\, \mathrm{d}y \tag{26}$$

The proper choice of each coefficient in the admissible function for minimizing the functional can be found by the following equation:

$$\frac{\partial L_{\max}}{\partial A_{ij}} = 0 \tag{27}$$

The preceding equation yields an $(I+1)(J+1)$ order eigenvalue problem. By solving the eignevalue problem, one can obtain $(I+1)(J+1)$ number of nondimensional frequency parameters and the corresponding mode shapes. One immediately discovers that the lower nondimensional frequencies and mode shapes are more accurate than the higher ones and tend to approach to the exact values as the number of terms in the admissible function are increased. The nondimensional frequency parameters are written in Table 2. UDNC will be employed on approximated mode shapes according to the following scope. UDNC will be applied up to the for a SS-C-SS-C rectangular plate. The selected dimension of the plate is 1×0.5 units. Applying the methodology outlined in Sec. III to the approximated mode shapes gives the locations of the actuator/sensor pairs:

$$x1 := 0.4978337, \qquad x2 := 1.0000000, \qquad x3 := 1.5021662$$
$$y1 := 0.3540555, \qquad y2 := 0.6459444 \tag{28}$$

As just presented, the locations are slightly different from the exact locations obtained by the analytical method. Applying the UDNC procedure presented in the preceding analytical case, the gain matrix is calculated by using the approximated mode shapes as follows:

$$G = g \begin{bmatrix} 27.497490 & 1.7099e^{-14} & 0 & 0 & 0.144993 & 0 \\ 1.7099e^{-14} & 28.725208 & 0 & 0 & 0 & -0.150819 \\ 0 & 0 & 27.567173 & 1.9180e^{-14} & 0 & 0 \\ 0 & 0 & 1.9180e^{-14} & 28.497885 & 0 & 0 \\ 0.144993 & 0 & 0 & 0 & 27.607363 & 2.1934e^{-14} \\ 0 & -0.150819 & 0 & 0 & -2.1934e^{-14} & 28.144987 \end{bmatrix} \tag{29}$$

The gain matrix is almost identical to the gain matrix obtained by analytical method, and the preceding gain matrix is approximately diagonal. Errors introduced by the approximation method (Ritz method) upon the mode shape, natural frequencies, and gain matrix are less than 1%.

Conclusions

In this study we have presented a methodology for uniform modal damping of plates with certain boundary conditions. The sensor actuator pairs are placed at the intersection of the nodes of the $(M+1)$ and $(N+1)$ mode. The method shows the following: 1) all modes are damped uniformly; 2) the open-loop and closed-loop frequencies are the same; and 3) the mode shapes are invariant. This methodology has been shown to work in all cases where the nodal lines intersect. If one were to examine the total number of simple boundary conditions (clamped, SS, free) for rectangular plates, one would find that there are 21 different combinations. The UDNC method works for all combinations except the following: C-F-S-F, C-F-C-F, S-F-S-F, C-F-F-F, S-F-F-F, F-F-F-F. In these cases there are no intersections of the nodal lines. A general solution for these cases remains elusive.

References

[1]Meirovitch, L., and Baruh, H., "Control of Self-Adjoint Distributed-Parameter Systems," *Journal of Guidance, Control, and Dynamics*, Vol. 5, No. 1, 1982, pp. 60–66.

[2]Meirovitch, L., and Baruh, H., "Robustness of the Independent Modal-Space Control Method," *Journal of Guidance, Control, and Dynamics*, Vol. 6, No. 1, 1983, pp. 20–25.

[3]Silverberg, L., "Uniform Damping Control of Spacecraft," *Journal of Guidance, Control, and Dynamics*, Vol. 9, No. 2, 1986, pp. 221–227.

[4]Weaver, L., and Silverberg, L., "Node Control of Uniform Beams Subject to Various Boundary Conditions," *Journal of Applied Mechanics*, Vol. 59, Dec. 1992, pp. 983–990.

[5]Washington, G., and Silverberg, L., "Uniform Damping and Stiffness Control of Structures with Distributed Actuators," *Journal of Dynamic Systems, Measurement and Control*, Vol. 119, 1997, pp. 561–565.

[6]Rossetti, D., and Sun, J., "Uniform Modal Damping of Rings by an Extended Node Control Theorem," *Journal of Guidance, Control, and Dynamics*, Vol. 19, No. 2, 1995, pp. 373–375.

[7]Silverberg, L., "Conjecture About Orthogonal Functions," *Journal of Guidance, Control, and Dynamics*, Vol. 20, No. 1, 1997, pp. 198–202.

[8]Hendry, S., "Comment on 'Conjecture About Orthogonal Functions'," *Journal of Guidance, Control, and Dynamics*, Vol. 21, No. 1, 1998, pp. 188–190.

[9]Lee, C., and Moon, F., "Modal Sensors/Actuators," *Journal of Applied Mechanics*, Vol. 57, 1990, pp. 434–441.

[10]Tzou, H., and Hollkamp, J., "Collocated Independent Modal Control with Self-Sensing Orthogonal Piezoelectric Actuators (Theory and Experiment)," *Smart Materials and Structures*, Vol. 3, 1994, pp. 277–284.

[11]Burke, S., and Hubbard, J., "Spatial Filtering Concepts in Distributed Parameter Control," *Journal of Dynamic Systems, Measurement and Control*, Vol. 112, 1990, pp. 565–573.

[12]Leissa, A., *Vibration of Plates*, Acoustical Society of America, Sewickley, PA, 1973.

[13]Qatu, M.-S., "Free Vibration and Static Analysis of Laminated Composite Shallow Shells," Ph.D. Dissertation, Dept. of Engineering Mechanics, Ohio State Univ., Columbus, OH, 1989.

Errata

H_∞ Feedback for Attitude Control of Liquid-Filled Spacecraft

Jinlu Kuang and A. Y. T. Leung
University of Manchester, Manchester, England M13 9PL, United Kingdom

[J. Guidance 24(1), pp. 46–53 (2001)]

THE first sentence in the last paragraph of the second column on page 50 should read as follows:
"The control law $u_x = -(a\omega_x + b\beta_x)$, $u_y = -(a\omega_y + b\beta_y)$, $u_z = -(a\omega_z + b\beta_z)$ was proposed by Mortensen,[15] who proved that the closed-loop system for a rigid spacecraft without external disturbances is globally and asymptotically stable."

The statement on page 51 following Eq. (101) should read as follows:
"where $u_x = -(a\omega_x + b\beta_x)$, $u_y = -(a\omega_y + b\beta_y)$, and $u_z = -(a\omega_z + b\beta_z)$, in which the coefficients a and b are defined according to the polynomial equations (83) and (84) together with inequality (44)."
AIAA regrets the error.